

# Antisymmetric RMF Current Drive in FRCs

R. D. Milroy,<sup>1,2</sup> H. Y. Guo,<sup>1</sup> A. L. Hoffman,<sup>1</sup> and L. C. Steinhauer<sup>1</sup>

---

A major concern for Rotating Magnetic Field (RMF) current drive of an FRC is that a transverse magnetic field tends to open the field lines, thus compromising confinement. In recent FRC current drive experiments it was found that thermal confinement is much improved when an antisymmetric RMF is applied, rather than the usual symmetric RMF. A field line tracking analysis showed that with a combination of partial penetration and antisymmetric RMF, the field lines remain closed for larger ratios of  $B_{\phi}/B_e$  than was previously thought. In this paper the analysis is extended to more fully understand the boundaries of when and where the field lines are expected to remain closed when antisymmetric RMF current drive is applied to an FRC.

---

**KEY WORDS:** Field reversed configuration; rotating magnetic field.

## INTRODUCTION

Rotating Magnetic Fields (RMF) can be used to both form and sustain Field Reversed Configurations (FRC). However the addition of even a small transverse magnetic field to an FRC tends to open the field lines, leading to a concern that confinement could be compromised. Calculations show that both electron and ion orbits are confined due to the cyclic nature of the field line opening [1,2], but rapid electron thermal conduction remains a concern unless the edge density can be maintained extremely low. It was shown [3] that if an antisymmetric RMF is applied, the field lines remain closed for small ratios of vacuum RMF  $B_{\phi}$  to external axial magnetic field  $B_e$ . Recent experiments show improved confinement when antisymmetric RMF is applied, and an analysis of these results [4] shows that field lines remain closed for much larger ratios of  $B_{\phi}/B_e$  due to the fact that the RMF only partially penetrates the FRC, and the

radial component of the RMF is lowered significantly from the vacuum value.

## THE MODEL

In this paper, the analysis of Guo *et al.* [4] is extended to include a representation of the antisymmetric RMF that more accurately accounts for the antenna geometry and FRC shape. This new model is used to map when and where field lines open, to determine the threshold for the opening of field lines, and to study the sensitivity of the results to precise symmetry.

Experimentally, an antisymmetric RMF is produced with a coil set similar to that shown in Figure 1. This figure shows the single coil set used to produce a magnetic field in the  $y$ -direction. Current flows in opposite directions in the upper and lower coil sets (heavy lines) producing a magnetic field in the  $+y$ -direction in the top half of the figure, and in the  $-y$ -direction in the lower half of the figure. The lighter lines are the magnetic field lines in vacuum, i.e. in the absence of plasma. An identical coil set, rotated  $90^\circ$  is used to produce a magnetic

<sup>1</sup> Redmond Plasma Physics Laboratory, University of Washington, Seattle, WA, 98195, USA.

<sup>2</sup> To whom correspondence should be addressed. E-mail: milroy@aa.washington.edu.

field in the  $x$ -direction. The current to produce the field in the  $x$ -direction oscillates  $90^\circ$  out of phase with the current to produce the field in the  $y$ -direction, resulting in a RMF.

The magnetic field model assumed in this paper is a superposition of the poloidal field from a 2D FRC equilibrium, and an analytic partially penetrated  $n = 1$  profile to represent the RMF. The poloidal field is derived by running the Moqui initial value MHD code until it comes to a quasi-equilibrium. An analytic partially penetrated  $n = 1$  profile derived by Hoffman [5] is added to the poloidal field in a similar manner to that of Guo *et al.* [4]. The equilibrium, along with the magnitude of the superimposed RMF as a function of  $z$  is illustrated in Figure 2.

In the previous work the RMF had no accompanying  $n = 1$  component to the axial magnetic field. The antennas employed in the experiments have current returns at the ends and at the midplane that produces a  $B_z$  component comparable to the  $B_\theta$  component as seen in Figure 1. In these calculations a  $B_z$  component is added; its magnitude is assumed to be proportional to  $\partial_z B_\theta$ , and the  $n = 1$  component of  $B_r$  is adjusted appropriately to preserve  $\nabla \cdot \mathbf{B} = 0$ .

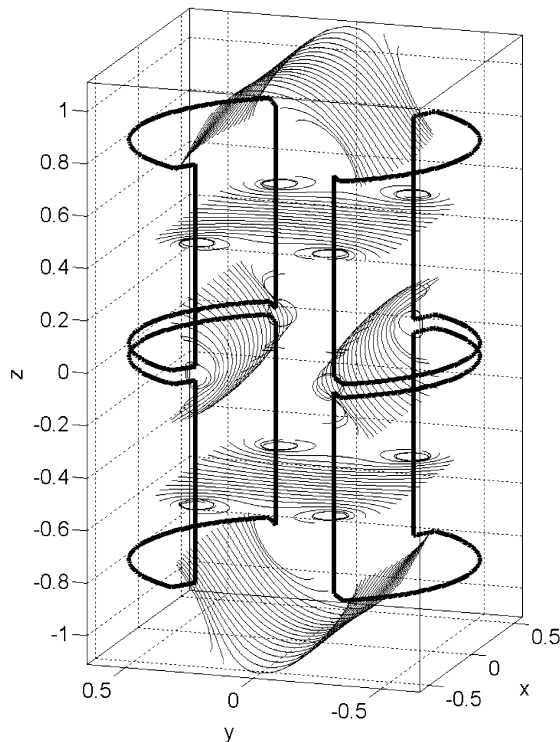


**Fig. 1.** Antenna geometry and selected field lines for antisymmetric RMF.

This is illustrated in Figure 3, which shows vector plots in the  $r$ - $z$  plane ( $\theta = \pi/2$ ) for the imposed RMF field.

In Ref. [5], the penetration depth of the RMF is specified with the parameter  $\delta^*/r_s$ . Here we hold  $\delta^*$  constant, so the ratio increases as  $r_s$  gets smaller. A cross section of the partially penetrated RMF field lines is plotted at three different axial locations in Figure 4. In the end regions, where the local  $r_s$  is small, the RMF is fully penetrated.

First, we look at a case where a symmetric RMF is applied.

## RESULTS

As a standard case we assume a penetration depth given by  $\delta^*/r_s = 0.15$  at the midplane, and an RMF magnitude given by  $B_{\omega}/B_{z0} = 0.25$ , where  $B_{\omega}$  is the RMF magnitude far from the plasma, and  $B_{z0}$  is the external axial magnetic field strength (from the equilibrium poloidal field) at the midplane. These parameters are typical for the TCS experiment. To evaluate whether or not a field line is open, we use a line tracing algorithm to measure how long it is before it intersects the wall. If a field line is found to extend more than  $100 \cdot r_s$  in both directions from a midplane starting point, it is assumed to be closed. If it intersects a wall, it is assigned a length equal to the shorter of the two distances. Field lines are started on a polar grid extending from  $r = 0$  to  $r = 1.5 \cdot r_s$ , with 40 points in the radial direction and 100 points in the  $\theta$ -direction.

Figure 5 shows contours of field line length as a function of their starting position in the  $x$ - $y$  plane (at the axial midplane) for a calculation with an axially symmetric RMF profile. Here it is found that all of the field lines open, and have a maximum length of about  $15 \cdot r_s$ . The circle with a radius of 1 indicates the position of the separatrix when no RMF is applied.

Figure 6 shows the results from an identical calculation, except that an antisymmetric RMF field is assumed. The length scale is from 0 to  $20 \cdot r_s$ , but all of the field lines that reached  $20 \cdot r_s$ , in fact had a full length of  $100 \cdot r_s$ . Thus, we find that almost all of the field lines are in fact closed for this case.

The calculation of Figure 6 assumes perfect symmetry in the FRC and RMF; something that is difficult to achieve experimentally. The sensitivity of these results to symmetry can be estimated by performing calculations with the imposed RMF shifted axially relative to the FRC. Results from

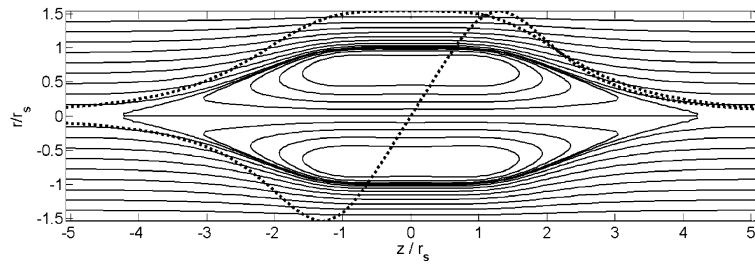


Fig. 2. Equilibrium flux surfaces, with the relative RMF magnitude (for both symmetric and antisymmetric profiles) as a function of  $z$  superimposed.

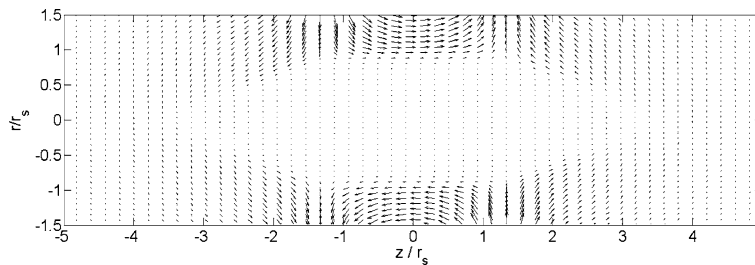


Fig. 3. Vector plots illustrating the antisymmetric RMF field in the plane of the external RMF.

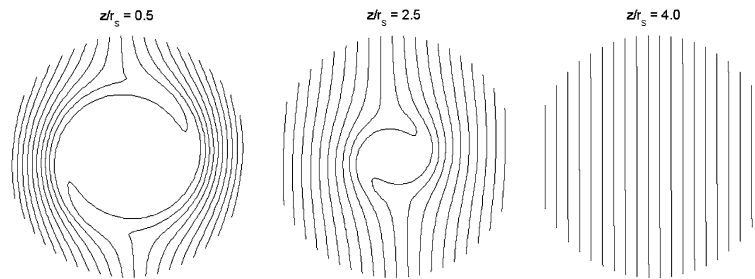


Fig. 4. RMF field lines at 3 different axial locations, illustrating partial penetration evolving to full penetration at the ends as  $r_s$  gets smaller.

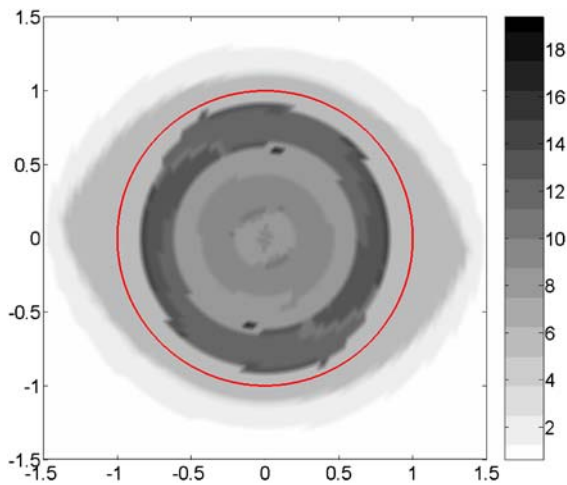


Fig. 5. Contours of field line length in units of  $r_s$  for a calculation with axially symmetric RMF.

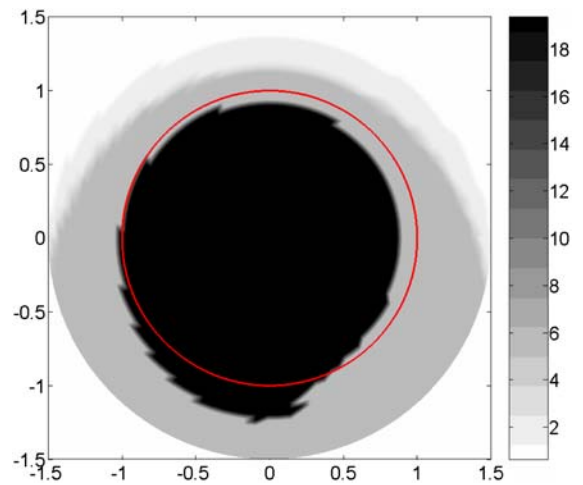


Fig. 6. Contours of field line length for a calculation with antisymmetric RMF.

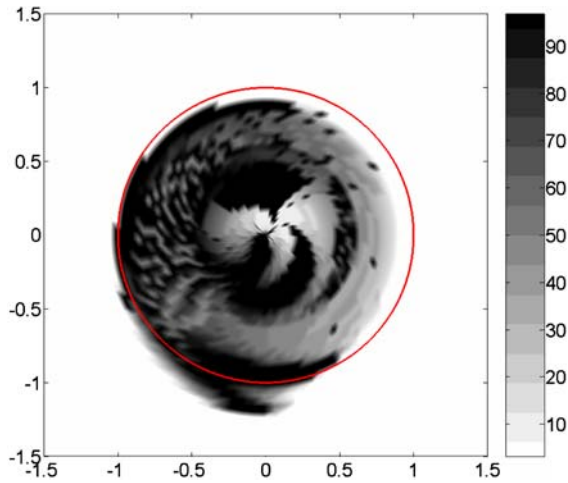


Fig. 7. Contours of field line length for a calculation with antisymmetric RMF and an axial shift of the RMF of  $r_s/6$ .

calculations with the RMF shifted axially by a distance of  $r_s/6$  are shown in Figure 7. Note that in this figure the contours are scaled for a range of 0–100, since it is found that for these conditions field lines open after traversing a considerable length in the FRC. This asymmetry opens many field lines, but they are much longer than those from the symmetric calculations. Furthermore, it should be noted that if the longer field lines allow the plasma to get hotter, and the ratio of  $B_\omega/B_{z0}$  is reduced to 0.10, a similar calculation shows that almost all of the field lines are then closed.

Finally, we have investigated the effect of adding a small amount of toroidal field to the FRC. The toroidal field magnitude is assumed to be  $B_\theta = B_{\theta 0} \psi / (r\psi_0)$  where  $\psi_0$  is the flux at the magnetic null and  $B_{\theta 0} = 0.25 \cdot B_{z0}$ . Ryutov *et al.* [6] found that the addition of even a weak toroidal magnetic field to a zero toroidal magnetic field system can reduce the radial excursions resulting from field perturbations. The spontaneous generation of toroidal magnetic fields has been observed in the TCS experiment [7]. Figure 8 shows the results of an identical calculation to that of Figure 7, except that a small toroidal field is added. Here we see a dramatic improvement in field line closure, with only a small hole near  $r = 0$ .

## CONCLUSIONS

These calculations are very encouraging for the RMF current drive program. The construction of

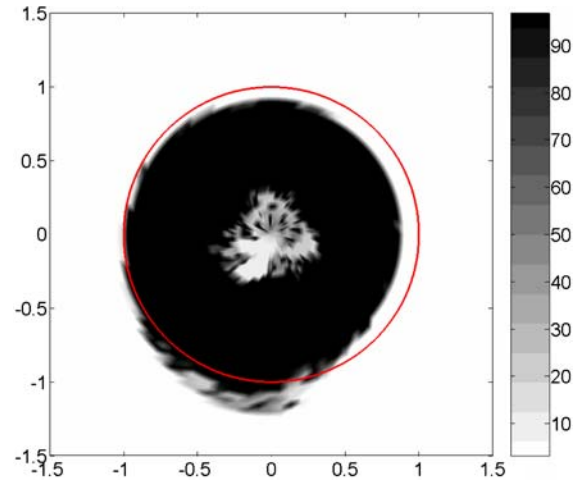


Fig. 8. Contours of field line length for a calculation with antisymmetric RMF, an axial shift of the RMF of  $r_s/6$ , and added  $B_\theta$ .

TCS upgrade experiment is nearing completion. This experiment employs good vacuum hygiene to reduce the impurity level and allow for higher temperatures and thus lower ratios of  $B_\omega/B_{z0}$ . In addition the experiment has been designed to employ an antenna set that will generate the antiparallel RMF. It has been shown here that the partial penetration allows the field lines to remain closed for much higher amplitude RMF than previously predicted for full penetration [3]. It is also found that the addition of a modest amount of toroidal field improves field closure dramatically. It is hoped that this combination will lead to a closed field configuration and high plasma temperatures.

## REFERENCES

1. W. N. Hugrass, and I. R. Jones, *J. Plasma Phys.*, **29**, 155 (1983).
2. W. N. Hugrass, and M. Turley, *J. Plasma Phys.*, **37**, 1 (1987).
3. S. A. Cohen, and R. D. Milroy, *Phys. Plasmas*, **7**, 2539 (2000).
4. H. Y. Guo, A. L. Hoffman, and L. C. Steinhauer, *Phys. Plasmas*, **12**, 062507 (2005).
5. A. L. Hoffman, *Nucl. Fusion*, **40**, 1523 (2000).
6. D. D. Ryutov, J. Kesner, and M. E. Mauel, *Phys. Plasmas*, **11**, 2318 (2004).
7. A. L. Hoffman, H. Y. Guo, K. E. Miller, and R. D. Milroy, *Nucl. Fusion*, **45**, 176 (2005).